

# **Numerische Untersuchungen von Massenstrom- und Temperaturverteilung, sowie des Wärmeübergangs in Plattenwärmeübertragern**

Von der Fakultät Energietechnik der Universität Stuttgart  
zur Erlangung der Würde eines Doktors der  
Ingenieurwissenschaften (Dr.-Ing.) genehmigte Abhandlung

vorgelegt von  
**Holger Rebholz**  
aus Stuttgart

|                             |                                     |
|-----------------------------|-------------------------------------|
| Hauptberichter:             | Prof. Dr.-Ing. E. Hahne             |
| Mitberichter:               | Prof. Dr.-Ing. H. Müller-Steinhagen |
| Tag der mündlichen Prüfung: | 18. Juli 2003                       |

**Institut für Thermodynamik und Wärmetechnik**

**2003**

## Inhaltsverzeichnis

|   | Seite     |
|---|-----------|
| Inhaltsverzeichnis  | 1         |
| Nomenklatur   | 3         |
| Kurzfassung   | 6         |
| Abstract  | 7         |
| <b>1. Einleitung</b>  | <b>19</b> |
| 1.1 Allgemeines   | 19        |
| 1.2 Stellung der Strömungssimulation in der Wissenschaft                    | 20        |
| 1.3 Problemstellung   | 21        |
| <b>2. Literaturübersicht</b>  | <b>24</b> |
| 2.1 Literatur zur thermischen Auslegung von Plattenwärmeübertragern         | 24        |
| 2.2 Literatur zur Massenstromverteilung auf parallele Kanäle                | 27        |
| 2.3 Literatur zum Einfluss von Prägungen auf die Strömung im Kanal          | 28        |
| <b>3. Theoretische Grundlagen</b>   | <b>31</b> |
| 3.1 Beziehungen aus der Wärmeübertragung                                    | 31        |
| 3.2 Definition der Kenngrößen im Kanal                                      | 34        |
| 3.3 Strömungsgleichungen und Turbulenzmodelle                               | 37        |
| <b>4. Der Plattenwärmeübertrager – Aufbau und Funktion</b>                  | <b>45</b> |
| 4.1 Einführung  | 45        |
| 4.2 Aufbau von Plattenwärmeübertragern                                      | 46        |
| 4.3 Der Kanal   | 47        |
| 4.3.1 Der Bereich der Hauptwärmeübertragungsfläche                          | 48        |
| 4.3.2 Das Verteilersegment  | 53        |
| 4.4 Verschaltungsarten von Plattenwärmeübertragern                          | 54        |
| <b>5. Das Computerprogramm für Thermische Berechnungen (CTB)</b>            | <b>60</b> |
| <b>- Aufbau und Validierung</b>   |           |
| 5.1 Die Beschreibung des Computerprogramm für Thermische Berechnungen (CTB) | 63        |
| 5.1.1 Automatische Geometrieerstellung                                      | 64        |
| 5.1.2 Automatische Gittererstellung   | 65        |
| 5.1.3 Diskretisierung und Lösen der Berechnungsgleichungen                  | 68        |
| 5.1.4 Beschreibung des Wärmeübergangs zwischen Kanal und Platte             | 71        |
| 5.1.5 Automatische Zuordnung der verschiedenen Blockeigenschaften           | 73        |
| 5.1.6 Automatische Zuordnung der Randbedingungen                            | 73        |
| 5.2 Validierung des Computerprogramm für Thermische Berechnungen (CTB)      | 77        |
| 5.2.1 Validierung 1: Das Graetz-Nusselt-Problem                             | 77        |
| 5.2.1.1 Problembeschreibung   | 77        |
| 5.2.1.2 Ergebnisse  | 79        |
| 5.2.2 Validierung 2: Freie Konvektion in einem Quadrat                      | 82        |
| 5.2.2.1 Problembeschreibung   | 83        |
| 5.2.2.2 Ergebnisse  | 83        |

|            |  |            |
|------------|--|------------|
| 5.2.3      | Validierung 3: Wärmeübergang zwischen Fluid und Festkörper   | 86         |
| 5.2.3.1    | Problembeschreibung  | 86         |
| 5.2.3.2    | Ergebnisse   | 87         |
| <b>6.</b>  | <b>Untersuchungen von Plattenwärmeübertragern mit dem Computerprogramm für Thermische Berechnungen (CTB)</b> | <b>90</b>  |
| 6.1        | Der Einfluss des Randeffekts auf die dimensionslose Temperaturänderung                                       | 90         |
| 6.1.1      | Der Einfluss des Gitters auf die Temperaturänderung  | 95         |
| 6.1.2      | Der Einfluss der Reynolds- und Prandtl-Zahl auf die Temperaturänderung                                       | 96         |
| 6.2        | Der Einfluss des Gleichstromeffekts auf die dimensionslose Temperaturänderung                                | 99         |
| 6.3        | Vergleich der dimensionslosen Temperaturänderung von Schaltungen   | 103        |
| 6.3.1      | Untersuchungen für $Re = 50$ und $Pr = 4,5$  | 104        |
| 6.3.2      | Untersuchungen für $Re = 150$ und $Pr = 4,5$   | 105        |
| 6.3.3      | Untersuchungen für $Re = 50$ und $Pr = 25$   | 106        |
| 6.3.4      | Untersuchungen für $Re = 150$ und $Pr = 250$   | 107        |
| 6.4        | Der Einfluss des Anstellwinkels auf die dimensionslose Temperaturänderung                                    | 109        |
| 6.4.1      | Untersuchungen für einen Anstellwinkel $\varphi = 90^\circ$  | 109        |
| 6.4.2      | Untersuchungen für Anstellwinkel $\varphi < 90^\circ$  | 112        |
| 6.4.2.1    | Untersuchungen laminarer Strömungen mit $0 < \varphi < 60^\circ$   | 114        |
| 6.4.2.2    | Untersuchungen turbulenter Strömungen mit $\varphi = 60^\circ$   | 117        |
| <b>7.</b>  | <b>Untersuchungen zur Temperaturverteilung im Umlenkungsbereich mit dem kommerziellen Programm FLUENT</b>    | <b>120</b> |
| 7.1        | Beschreibung der Geometrie   | 120        |
| 7.2        | Beschreibung der Gitter  | 122        |
| 7.3        | Ergebnisse   | 123        |
| 7.3.1      | Der Einfluss des Gitters auf die Austrittstemperaturen   | 124        |
| 7.3.2      | Der Einfluss unterschiedlicher Interpolationsverfahren auf die Austrittstemperaturen                         | 125        |
| 7.3.3      | Untersuchungen laminarer Strömungen mit $w = 0,01$ m/s   | 125        |
| 7.3.4      | Untersuchungen turbulenter Strömungen mit $w = 1$ m/s  | 128        |
| <b>8.</b>  | <b>Untersuchungen zur Massenstromverteilung im Verteilersegment mit dem kommerziellen Programm FLUENT</b>    | <b>131</b> |
| 8.1        | Beschreibung der Geometrie   | 132        |
| 8.2        | Beschreibung der Gitter  | 135        |
| 8.3        | Ergebnisse   | 136        |
| 8.3.1      | Der Einfluss des Gitters auf die Massenstromverteilung   | 137        |
| 8.3.2      | Der Einfluss des Druckverlusts im wärmeübertragenden Bereich auf die Massenstromverteilung                   | 137        |
| 8.3.3      | Der Einfluss der Eintrittsgeschwindigkeit auf die Massenstromverteilung                                      | 139        |
| <b>9.</b>  | <b>Zusammenfassung</b>   | <b>143</b> |
| <b>10.</b> | <b>Literaturverzeichnis</b>  | <b>148</b> |
| <b>11.</b> | <b>Anhang</b>  | <b>152</b> |

## Kurzfassung

Im Rahmen dieser Arbeit werden die Methoden der numerischen Strömungsmechanik auf die Thematik der Plattenwärmeübertrager angewandt. Dabei ist einerseits die Auslegung gesamter Plattenwärmeübertragerschaltungen (Kap.6) von Interesse, andererseits die Untersuchung lokaler Strömungsverhältnisse in Teilbereichen eines Plattenwärmeübertragers (Kap.7 und Kap.8).

Durch Anwendung der CFD-Methode (Computational Fluid Dynamics) können Plattenwärmeübertragerschaltungen ohne die Angabe eines Wärmedurchgangskoeffizienten berechnet werden. Zur Realisierung wird das eigene Computerprogramm für Thermische Berechnungen (CTB) entwickelt, welches speziell an die Anwendung auf Plattenwärmeübertrager angepasst ist. Dies beinhaltet eine automatische Geometrieerstellung des Strömungsbereichs, eine automatische Gittergenerierung mit lokaler Auflösung der wandnahen Bereiche und eine automatische Zuordnung der Randbedingungen für die Vielzahl von Schaltungsvarianten. Zur Validierung des Programms werden die analytische Lösung des Graetz-Nusselt-Problems, sowie detailliert untersuchte numerische Testbeispiele aus Literaturstellen herangezogen. Es wird das Temperaturverhalten unterschiedlicher Schaltungsvarianten berechnet, sowie die Einflüsse der Rand- und Gleichstromeffekte auf die dimensionslose Temperaturänderung untersucht. Vergleiche mit anderen Forschungsarbeiten zeigen eine gute Übereinstimmung. Zusätzlich erfolgt eine Anpassung des Programms für die quantitative Berechnung von Plattenwärmeübertragern. Neue Erkenntnisse über die lokalen Strömungsverhältnisse zeigen gerichtete Strömungen in den komplizierten Kanalgeometrien. Diese Strömungen in den Talern der Plattenprägungen sind durch einen geringen Wärmeübergang charakterisiert und ähneln Strömungen in ebenen Kanälen. Es wird eine effektive Plattenlänge in Abhängigkeit vom Anstellwinkel der Prägungen definiert. Die Theorie ist für laminare Strömungsverhältnisse bei kleinen Anstellwinkeln geeignet. Für größere Geschwindigkeiten bzw. höhere Anstellwinkel induzieren die Talströmungen Schubspannungen, welche zu Sekundärströmungen führen. Diese Sekundärströmungen dominieren den Wärmeübergang und werden im Programm CTB über Turbulenzfaktoren wiedergegeben.

Im zweiten Teil dieser Arbeit wird die thermische Vermischung im Umlenkungsbereich mehrgängiger Schaltungen untersucht. Für kleine Geschwindigkeiten ergibt sich bei 5 parallelen Kanälen je Durchgang keine vollständige Vermischung, bei höheren Geschwindigkeiten hingegen ist mit fast einheitlichen Temperaturen zu rechnen. Des Weiteren wird die Massenstromverteilung in einem Verteilersegment berechnet. Je nach Rückwirkung des Druckverlusts im wärmeübertragenden Bereich ergeben sich unterschiedliche Massenstromverteilungen am Eintritt in den wärmeübertragenden Bereich. Mit größer werdendem Anstellwinkel der Prägungen im wärmeübertragenden Bereich wird die Ungleichverteilung verringert. Es wird der Einfluss unterschiedlicher Eintrittsgeschwindigkeiten auf die Massenstromverteilung untersucht.

## Abstract

The present work applies the CFD-method (Computational Fluid Dynamics) to Plate Heat Exchangers (PHEs) to obtain more accurate solutions for the design of PHEs and gain a better understanding of the fluid flow in the complex channels. Therefore the study is divided into two sections. The main part deals with the development of a new program CTB, which can be applied to the design of PHEs. The second part focuses on the local nature of the fluid flow in PHEs. The thermal mixing in between two passes is investigated. Furthermore the fluid flow in the entrance region (header) of a single channel is calculated using the CFD-method. The main goal is to prevent a maldistribution, otherwise a negative influence on the heat transfer in the exchanger core occurs.

## A.1 Numerical Investigation of Plate Heat Exchanger Design

### A.1.1 Introduction to Plate Heat Exchanger Design

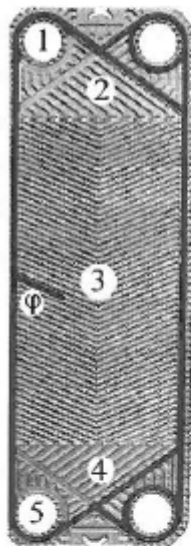


Fig.1':Corrugated Plate

A typical corrugated plate is shown in fig 1'. The fluid enters through the inlet port (1) and distributes throughout the header segment (2). The following region is called the main heat transfer surface (3), finally the fluid reaches the outflow segment (4) and exits through the outlet port (5). The angle  $\varphi$  is defined between the main flow direction and the corrugations. Plate Heat Exchangers (PHEs) are used in a wide range of applications within the fields of engineering. Although PHEs have several advantages in comparison to other types of heat exchangers, difficulties exist in determining the best flow configuration, as well as understanding the thermal behaviour of the selected PHE arrangement. The prediction of the temperature field in PHE design is very important for classifying the arrangement. It must be decided what kind of arrangement for a given mass flow guarantees the maximum heat duty under consideration of the pressure drop. Parameters are the total number of channels for each fluid and the number of passes for each fluid. Many

PHE arrangements are poorly designed with little effort to guarantee thermal efficiency and low cost. To ensure the heat duty, PHEs are often oversized and cost more than arrangements with the same heat duty and fewer plates. For achieving a more detailed design process, Computational Fluid Dynamics (CFD) is a most effective tool. Heat Exchanger design methods were published in the 1950s for a wide range of operating conditions, without using a uniform

description. This makes it difficult to compare these methods. Bosnjakovic et. al. (1951) began to avoid these problems by defining the characteristic  $\Phi$ . This characteristic sets up a connection between the inlet and outlet temperatures of heat exchangers. Difficulties arise in determining this characteristic, because it varies for different arrangements. For common flow configurations, such as pure parallel flow, counterflow or cross flow it is published in the literature.

Many investigations followed with having simplifications mentioned by Hewitt et. al. (1994).

- The use of a constant overall heat transfer coefficient is not accurate, particularly in laminar flow. The inflow effects and the development of the boundary layers play a specific role.
- End effects are neglected, or simply implemented through a correction factor. These become important for PHE arrangements of less than 40 plates.
- The heat conduction in the fluid and in the plate in direction of the flow cannot be taken into account.
- Uniform velocities and temperatures in the channels and plates are assumed, thus the profiles in the channels and the distribution in the plates are neglected.

All methods and their results depend on the accurate determination of the overall heat transfer coefficient. If this is not well prescribed then the calculation results will be inaccurate. The overall heat transfer coefficient is calculated with correlations, which are obtained from experiments. The approximation of the overall heat transfer coefficient can be avoided, provided the fluid flow is also part of the calculation. This goal can be achieved by using the tool of Computational Fluid Dynamics. Due to the need for fast results, simplifications in geometry are necessary. Otherwise the time needed for grid generation would result in a very expensive outcome. Therefore a two-dimensional approach has been used for laminar fluid flow in this work.

### A 1.2 Numerical Approach

The flow is calculated two-dimensionally with velocity components  $u$  and  $v$  along the  $x$  and  $y$  coordinates. The flow is incompressible, and all fluid properties are constant. Heating through viscous dissipation and compression work is neglected. No internal heat generation is present in the solid or in the fluid. The conservation equations for mass, momentum and energy (Eqs. (1')-(3')) are solved in their integral form. The solutions are steady, the unsteady term is neglected.

$$\frac{\partial w_i}{\partial x_i} = 0 \quad (1')$$

$$\rho w_j \frac{\partial w_i}{\partial x_j} = -\frac{\partial p}{\partial x_i} + \mu \left( \frac{\partial^2 w_i}{\partial x_j^2} \right) \quad (2')$$

$$\rho w_i c_p \frac{\partial T}{\partial x_i} = k \frac{\partial^2 T}{\partial x_i^2} \quad (3')$$

In the solid the convective part is zero, and only the energy equation is solved. The governing equations were solved numerically using the control-volume-based finite-volume method. PHE geometries consist of very long and small ducts. This causes the following two numerical problems. First the multigrid approach causes difficulties. The calculation is based on three grids with non-uniform refinement, which are calculated one after the other from the coarse to the fine. Secondly, a discretisation of higher order in the region of the solid-fluid interfaces is not advisable, but rather a second order approach is recommended (Davis 1983). For the current work the first order discretisation is sufficient, and to avoid oscillations the Deferred Correction approach is used (Khosla and Rubin 1974). Because of the nonlinearity and the velocity-pressure coupling an iterative solution method is necessary. Therefore the SIMPLEC approach is used (van Doormal and Raithby 1984). To avoid numerical difficulties first the mass and momentum equations and then the energy equation are solved. For the computational domain multi-block partitions are used, one block for each fluid domain and one block for each solid domain.

The conjugate heat transfer between the solid-fluid-interface is solved applying the method described by Patankar (1980). This uses the harmonic mean of the solid and fluid thermal conductivities and other properties to derive a correct expression of the heat flux.

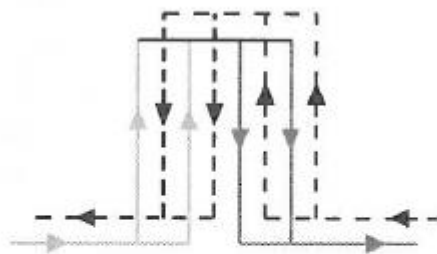


Fig. 2': 2-2 counterflow - counterflow arrangement

PHE arrangements are designed in different ways. The highest thermal effectiveness is achieved with pure counterflow arrangements. Therefore one should focus on the variety of those configurations. A PHE arrangement is determined by several parameters. The fluid is distributed throughout several channels, called a pass. The number of passes and the number of parallel channels for each fluid determine the size of the plate heat exchanger. For the flow configuration two more parameters must be named.

First the flow configuration in the channels and secondly the flow configuration of the whole plate heat exchanger. The second one only occurs in multipass arrangements. Fig. 2' shows a 2-pass arrangement with two channels per pass.

The geometry and the boundary conditions are automatically linked to the input parameters. These are the number of passes and parallel channels for each fluid and the description for counterflow or parallel-flow in the channels and the whole PHE. For the geometry the input parameters are channel width, plate thickness and plate length. The algorithm determines the inflow and outflow channels as well as the connecting faces between two following passes.

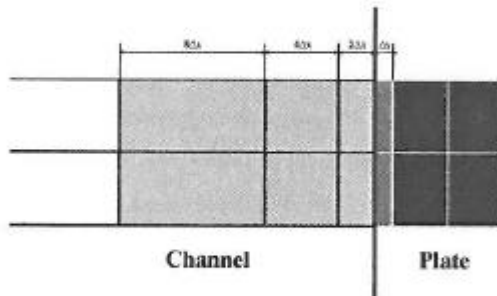


Fig.3a': Coarse Grid near Fluid-Solid Interface

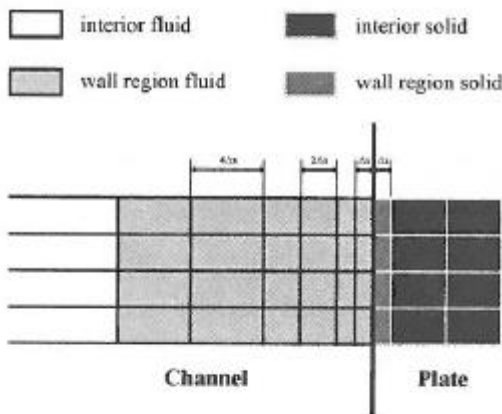


Fig.3b': Fine Grid near Fluid-Solid Interface

The grid is generated automatically. It is refined close to the fluid-solid interface to represent the correct heat flux. In order to avoid numerical difficulties and slower convergence, using too many control volumes in the solid should be avoided (fig.3a'). The next finer grid is obtained by non-uniform refinement (fig.3b'). In the fluid region each control volume is subdivided into four finer ones. In the solid the number of control volumes perpendicular to the flow direction remains constant, therefore resulting in just two fine control volumes. The cell shape is, due to the geometry of the calculated flat plates, always rectangular and therefore ideal to calculate the equations with a minimum of numerical diffusion. As it follows from the geometry of the long and narrow channels the aspect ratio becomes important. The ratio is a measure for the stretching of the cells. It can exceed 5:1, but only in highly anisotropic flows.

The mass flow is the same for each parallel channel. A great deal of research has been done for the manifold problem. However for plate heat exchangers the pressure drop in the channels is much higher than in the inflow- or outflow-header, respectively in-between passes. Therefore an equal distribution for the individual mass flow rates can be assumed. As a function of the pressure drop in the channels, the number of plates leading to maldistribution can exceed 100 (Kandlikar and Shah 1989/1).



### A 1.3 Results

The numerical program was validated by several benchmark solutions. Kaminski and Prakash (1986) published investigations on conjugate heat transfer. The comparison of their results with

Table 1': Overall Nusselt number at the solid-fluid interface

| Gr     | z  | Kaminski | CTB   |
|--------|----|----------|-------|
| $10^3$ | 5  | 0.87     | 0.87  |
|        | 25 | 1.02     | 1.02  |
|        | 50 | 1.04     | 1.04  |
| $10^4$ | 5  | 2.08     | 2.08  |
|        | 25 | 3.42     | 3.41  |
|        | 50 | 3.72     | 3.70  |
| $10^5$ | 5  | 2.87     | 2.86  |
|        | 25 | 5.89     | 5.87  |
|        | 50 | 6.81     | 6.78  |
| $10^7$ | 5  | 3.53     | 3.52  |
|        | 25 | 9.08     | 9.09  |
|        | 50 | 11.39    | 11.42 |

the numerical values of the program CTB is shown here, demonstrating the good agreement with all validations. The interior domain consists of a fluid region and a solid region. The heat transfer at the interface is part of the calculation. A comparison for the overall Nusselt numbers Nu at the interface as a function of the Grashof number Gr and a parameter z is shown in table 1'. The parameter z is defined in eq. (4'), with L as the width of the fluid region, t as the width of the solid region,  $k_w$  as the thermal conductivity of the wall and k as the thermal conductivity of the fluid.

$$z = \frac{k_w L}{k t} \quad (4')$$

Kandlikar and Shah (1989/2) mentioned that there are two effects in Plate Heat Exchangers leading to a decreasing heat duty between two fluids.

The first one is called the end effect, which occurs in every PHE arrangement. The channels at both ends of the PHE differ from the interior channels due to adiabatic wall conditions at the ends (heat transfer losses neglected). The second one occurs within multipass PHE arrangements. The plates between two adjacent passes have different flow configurations as compared to the plates within the adjacent passes. The influence of the two effects on the effectiveness is described in the following paragraphs.

*Single pass arrangement:* The end effect occurs due to the fact that the channels at both ends of the plate heat exchanger are heated from one side only. The fluid experiences a smaller temperature change than in the other parallel channels. Consequently there exists a higher temperature difference to the other fluid than in the interior, which leads to a higher temperature change in the adjacent channel. The ratio  $\Delta P_{real}/\Delta P_{ideal}$  describes the reducing influence of the end effect.

$\Delta P_{ideal}$  is the ideal temperature effectiveness of the fluid without end effects and is achieved in the interior of the Plate Heat Exchanger.

Kandlikar and Shah found that the end effect becomes insignificant when the number of plates exceeds 40. This is compared to calculations for a pure counter flow configuration and one pass. Fig. 4' shows, that with an increasing number of channels the end effect becomes less significant. For 20 channels of each fluid (equals 39 plates) the ratio  $\Delta P_{real}/\Delta P_{ideal}$  reaches 0.984. A ratio of one would require an infinite number of plates. The statement of Kandlikar and Shah (1989/1) can be confirmed.

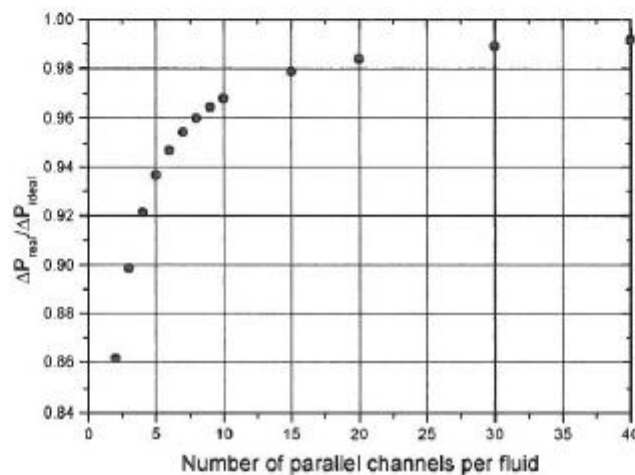


Fig. 4': End effect as a function of number of channels for a one-pass counterflow arrangement

*Multipass arrangements:* In multipass arrangements there is another effect occurring besides the end effect. The use of more than one pass leads to channels with different flow configurations compared to the other channels. This effect is investigated for a two-pass configuration and an overall counterflow arrangement of each stream in the channels and counterflow across the overall heat exchanger. The plates between these passes have parallel flow. The number of parallel channels is varied as for the single pass arrangement. Both effects – end effect and parallel flow effect between the adjacent passes – are occurring. In fig.5' the temperature change for each channel of Fluid 1 normalized by the maximum temperature change (channel 39), is shown (2-10 counterflow - counterflow). The end effect appears in the first and last pass. A reducing effect on the heat duty is also occurring due to the parallel flow. The outline of the temperature change distribution of each pass is the same. For Fluid 1 there is one channel in each pass with a

small temperature change ( 54.6% channel 1 – 53.4% channel 21) and on the other side of each pass a channel with a high temperature change (98.2% channel 19 – 100% channel 39).

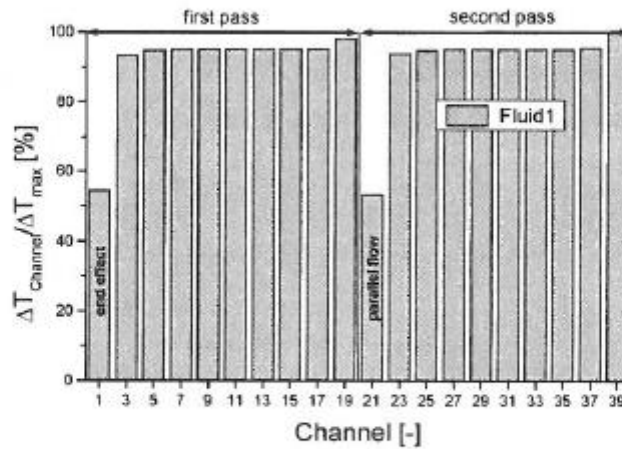


Fig. 5<sup>o</sup>: Temperature change in each channel for a 2-10 counterflow-counterflow arrangement

By variation of the number of channels for each pass, the end effect and the parallel flow effect have less significance. One has to keep in mind that the number of channels for each fluid has to be multiplied by two (two passes), and the number of channels for the complete arrangement has to be multiplied by four (two passes, two fluids). The arrangement with 20 channels per pass shows a ratio of 0.98 and the two effects can be neglected. Such an arrangement consists of 79 plates.

To find answers to the question of whether to design single or multipass arrangements, the result of several calculations will be shown. There are two contrary effects occurring, if the number of passes is increased. For the same mass flow and the same total number of channels, the velocity increases for multipass arrangements due to the reduced number of parallel channels per pass. Therefore the heat transfer coefficient  $h$  increases. On the other hand due to the parallel flow in between passes, the heat transfer is reduced compared to counterflow because of the reduced temperature difference.

To estimate how the two effects behave under several conditions, the 2D approach is used. Four conditions are investigated, with the Reynolds number and the Prandtl number being varied. The Reynolds number is given for the arrangement with one pass, and increases as the number of passes increases. The number of plates is fixed to 11, having 6 channels for each fluid. All arrangements have counterflow in the channels as well as in the complete plate heat exchanger.

Fig.6' shows the negative influence of the parallel flow configuration in between passes on the thermal performance. Under laminar conditions, the reduction of the heat duty due to the parallel flow channels overcomes the increase due to higher velocities. Even a velocity that is six times higher cannot compensate the reducing effect. This occurs in cases, when the temperature effectiveness per fluid is close to unity ( $P=1$ ), with the parallel flow being unable to reach 1 and therefore reducing the heat duty of the arrangement. Even if the effectiveness  $P$  is lowered to values around 0,4 by either increasing the Reynolds- or Prandtl number, the gain in pressure drop is to dominating compared to the increase of heat duty. Under laminar considerations the only application for multipass arrangements is found for high Prandtl-numbers (e.g. glucose solution).

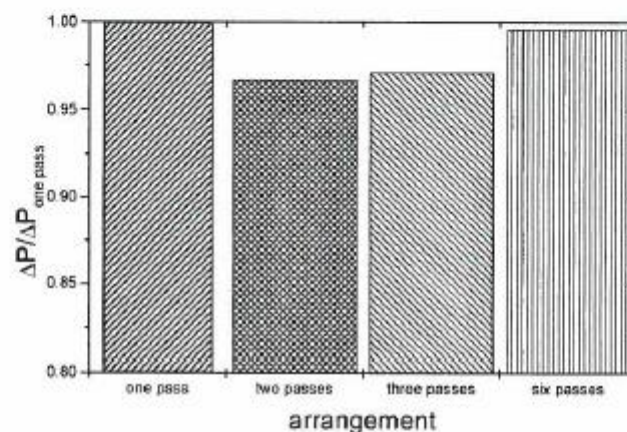


Fig.6': Comparison of the four arrangements for  $Re = 50$  (one pass) and  $Pr = 4.5$  (water)

The influence of the end effect as well as the influence of parallel flow between adjacent passes is investigated. Both effects are insignificant for a large number of plates. The end effect can be neglected for single pass arrangements with more than 39 plates (equals 2 percent reduction of effectiveness), while in arrangements with more than one pass the changing flow configuration leads to 79 plates (equals 2 percent reduction of effectiveness).

Similar to Kandlikar and Shah (1989/1), it was found, that one pass arrangements should be preferred over multi-pass arrangements as long as the flow distribution to the parallel channels is the same. Only for arrangements with a very low  $P$  value can the heat duty be increased significantly by the use of multiple passes.

The qualitative comparison with different flow arrangements in PHE design results in a very good agreement with literature data. Furthermore calculations of temperature fields in PHEs should also have quantitative accuracy. Therefore the nature of the fluid flow between the

corrugated plates is investigated in literature. Experimental investigations (Gaiser (1990), Heggs et. al. (1997)) show that a core of fluid flows along the troughs of the corrugations. These troughwise flows can be compared to fluid flow with little heat transfer in a flat channel. The two flows in the furrows of each plate must impose a shear stress on each other, inducing a swirling flow in the base of the corrugations. This secondary motion increases heat transfer and is very important for higher corrugation inclination angle (except  $\varphi = 90^\circ$ ). For small corrugation inclination angles the secondary motion is reduced, and a new theory of the increased plate length can be applied.

**Table 2':** Influence of the corrugation inclination angle on the heat transfer

| $\varphi$ | $j(\varphi)/j(30^\circ)$<br>Focke et.<br>al. (1985) | $L_{\text{eff}}(\varphi)/L_{\text{eff}}(30^\circ)$<br>Theory of<br>effective length |
|-----------|---|---|
| 0         | 0.85  | 0.87  |
| 30        | 1   | 1   |
| 45        | 1.28  | 1.22  |
| 60        | 1.73  | 1.73  |

This theory is based on the heat transfer equation. The product  $U \cdot A$  is increased due to the corrugation inclination angle  $\varphi$ . Instead of increasing the overall heat transfer coefficient  $U$ , the increased heat duty could also be due to increased stream length.

Eq. (5') shows the effective length as a function of the corrugation inclination angle.

$$L_{\text{eff}} = \frac{L}{\cos \varphi} \quad (5')$$

The factors of increased colburn factors (Focke et. al. (1985), normalised by the value for  $30^\circ$  are compatible to the factors for the effective length (Table 2'). For angles higher than  $60^\circ$  this theory is not valued anymore, due to the increased influence of swirling motion.

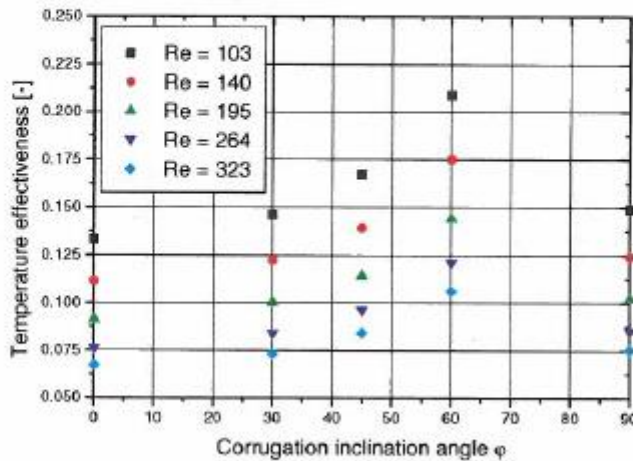


**Fig.7':** Dependency of the corrugation inclination angle on the temperature effectiveness



Fig. 7' shows the temperature effectiveness for 0°, 30°, 45°, 60° and 90°. It points out the common trend, determined by authors like Focke et. al. (1985) or Rosenblad and Kullendorf (1975) etc.

For corrugation inclination angles higher than 60° or higher velocities turbulent phenomena dominate the heat transfer and the laminar calculations fail. This is shown in fig. 8' for the laminar approach. A second theory is presented for turbulent conditions. Eq. (6') states the turbulence factor  $f_p$ . This model shows a good agreement with experimental data.

$$\dot{Q}_p = \int_A k \cdot \frac{\partial T}{\partial x} \cdot dA \approx \sum_N f_p \cdot k_n \cdot \frac{T_N - T_p}{x_N - x_p} \cdot A_n \quad (6')$$

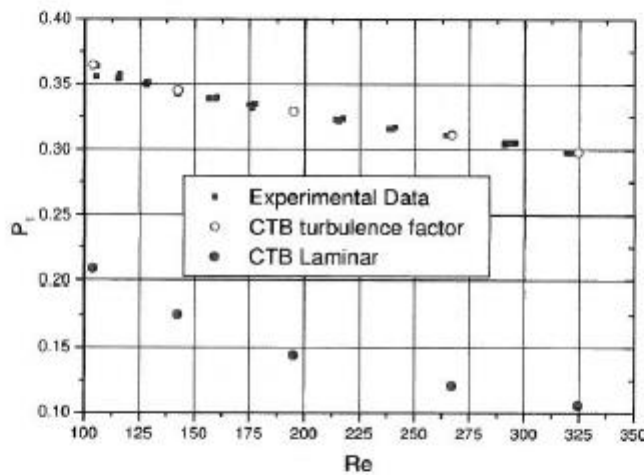


Fig.8': Temperature effectiveness for turbulent conditions

## A.2 Numerical Investigation of Local Fluid Flow in PHEs

### A.2.1 Simulation of a thermal mixing process in between two passes

In every pass a reduced temperature change in one channel occurs due to the end effect or the parallel flow effect. This leads to a thermal mixing process of several streams with different temperature in between two passes. For the modelling in Chapter A.1 it is essential to know, whether the distributed fluid flow on the next pass has equal temperature or a nonuniform temperature distribution. Variations for different inlet duct cross-sectional areas are calculated, as well as laminar and turbulent conditions. The arrangement consists of 5 channels per pass.

The investigations show that with laminar flow, a nonuniform temperature distribution for the fluid leaving the mixing zone occurs. As the diameter of the inlet and outlet ducts increases, the maximum temperature shifts towards the end of the mixing zone.

Fig. 9' shows the temperature distribution throughout the five channels for the smallest diameter of the inlet duct. With laminar flow the maximum temperature effectiveness occurs in the third outlet. For higher velocities and turbulent conditions the maximum moves towards the second outlet. The temperature distribution is almost uniform.

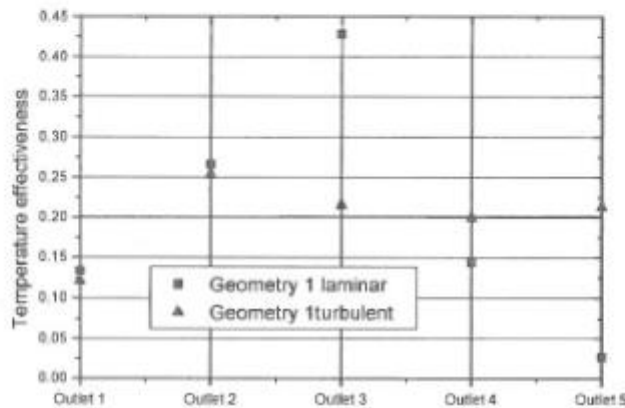


Fig.9': Temperature effectiveness at the outlets for laminar and turbulent conditions

## A 2.2 Investigation of fluid flow in the header segment of a plate heat exchanger

The main part of heat in a plate heat exchanger is transferred in the exchanger core. The thermal performance of this region is dependent on the flow distribution. The design of the header segment significantly affects this velocity distribution approaching the exchanger core. Therefore the major task of the header segment is to guarantee a uniform fluid distribution. An experimental optimisation of the header segment is very difficult, as it is focused on integral values like heat transfer and pressure drop, leaving a lack of understanding of the local flow patterns. By helping to understand the reasons for maldistribution, CFD can solve this problem.

A CAD-geometry of a header segment is discretized to obtain a numerical solution. The distribution is dependent on the pressure drop in the exchanger core. The pressure drop is modelled by a 2D-patch, flow simulations were done for laminar and turbulent conditions.

Fig. 10' shows the distribution for 0,1 m/s at the outlets of the header segment. Two different grids were calculated to obtain the influence of the control volume distribution on the results. Furthermore variations of the friction factor for the exchanger core show, that with an increasing corrugation angle the distribution becomes more uniform.

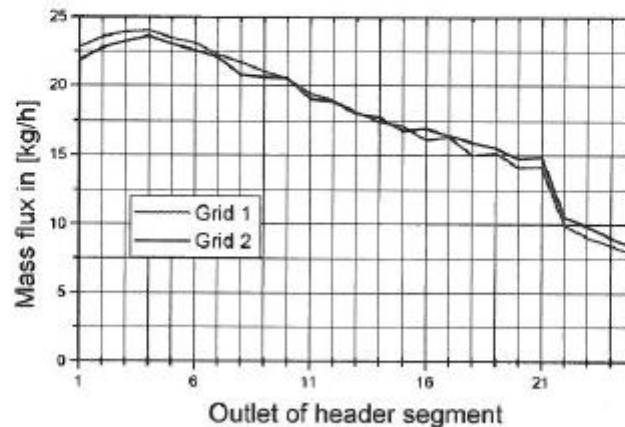


Fig.10': Non-uniform mass flux distribution approaching the exchanger core

### A.3 English Nomenclature

|                |   |
|----------------|---|
| A              | surface, m <sup>2</sup>                               |
| CFD            | Computational Fluid Dynamics                          |
| CTB            | Computerprogramm für Thermische Berechnungen          |
| f <sub>p</sub> | turbulence factor, dimensionless                      |
| Gr             | Grashof number, dimensionless                         |
| J              | Colburn factor, dimensionless                         |
| k              | thermal conductivity, W/m K                           |
| L              | Length of fluid region, m                             |
| p              | pressure, N/m <sup>2</sup>                            |
| P              | temperature effectiveness, dimensionless              |
| PHE            | Plate Heat Exchanger                                  |
| Q̇             | heat flow, W  |
| Re             | Reynolds number, wd <sub>h</sub> /ν, dimensionless    |
| t              | width of solid region, m                              |
| T              | temperature, K  |
| U              | overall heat transfer coefficient, W/m <sup>2</sup> K |
| w              | velocity, m/s   |
| x              | coordinates, m  |
| z              | Parameter see eq.(4'), dimensionless                  |

#### Greek symbols

|   |  |
|---|--|
| μ | dynamic viscosity, kg/m s                                  |
| φ | corrugation inclination angle to main flow direction, grad |
| ρ | density, kg/m <sup>3</sup>                                 |

#### Subscripts

|       |   |
|-------|---|
| eff   | effective length of PHE   |
| i     | summation index   |
| ideal | ideal temperature change without end effect or parallel flow effect |
| max   | maximum   |
| n     | control volume face between N and P                                 |
| N     | control volume center, neighbour volume of P                        |
| P     | control volume center   |
| real  | real temperature change due to end effect or parallel flow effect   |
| W     | wall  |